Asymmetric Visible-Light Photoredox Cross-Dehydrogenative Coupling of Aldehydes with Xanthenes.

Evgeny Larionov,[†] Marco M. Mastandrea,[†] and Miquel A. Pericàs[*,†,‡]

[†] Institute of Chemical Research of Catalonia (ICIQ), The Barcelona Institute of Science and Technology, Avda. Països Catalans, 16, 43007 Tarragona, Spain

[‡] Department de Química Organica, Universitat de Barcelona, 08080 Barcelona, Spain

Supporting Information Placeholder

ABSTRACT: We report a methodology for the catalytic asymmetric cross-coupling of two $C(sp^3)$–H bonds employing visible light as an economical and environmentally benign source of energy. Photoredox catalysis is used for the oxidation of a diarylmethane to the corresponding cation, which is then trapped by an enamine intermediate generated *in situ* from an aldehyde reactant and a secondary amine organocatalyst. Notably, this mild method is an ideal synthetic approach from the green chemistry point of view. It does not require preinstallation of functional groups, thereby constituting an atom economical, efficient transformation, and allows the formation of a C–C bond with simultaneous installation of one or two new stereocenters in a highly enantio- and diastereoselective manner. Mechanistic studies by experimental and computational methods aid to clarify the origin of the observed enantioselectivity.

Keywords: asymmetric catalysis, photoredox, coupling, mechanism, DFT, organocatalysis

The direct functionalization of inert C–H bonds has emerged in recent years as a powerful tool in synthetic organic chemistry.[1,2] The cross-dehydrogenative coupling (CDC) reaction of the C–H bond α to a nitrogen, oxygen or a carbonyl group represents one of the most successful examples of mild and selective C–C bond formations from C–H bonds.[3,4] Compared with non-asymmetric CDC reactions, only limited examples of enantioselective protocols for the C–C coupling *via* $C(sp^3)$–H activation have been reported so far.[5] Such a combination of dehydrogenative cross-coupling with asymmetric catalysis not only provides a fast increase of the structural complexity of a molecule, but also allows to install simultaneously one or multiple stereocenters.

In the past several years, due to its prominent energy-saving and environmentally benign features, visible-light photoredox catalysis has witnessed rapid development and attracted a great deal of interest in both academia and industry.[6,7] The synergetic combination of photoredox with other modes of catalytic activation has emerged as a powerful approach to discover novel reactivities and improve reaction conditions.[8] However, application of photoredox catalysis to asymmetric CDC reactions remains a formidable challenge, and few examples have been described in literature so far (Figure 1). Rovis and co-workers reported the combination of NHC-catalysis and visible light photocatalysis for the functionalization of tetrahydroisoquinolines (Figure 1a).[9a] Meggers group developed an enantioselective α-alkylation of ketones using a chiral at metal Rh-complex, which serves both as photoredox catalyst and chiral Lewis acid in this transformation (Figure 1b).[5d] Despite the great progress in enantioselective photoredox α-alkylation of aldehydes using alkyl bromides,[10]

there are few reports on the corresponding photoredox CDC reactions with non-functionalized $C(sp^3)$-H bonds.[11] We envisioned that the combination of enamine and photoredox catalysis would enable an asymmetric coupling between diarylsubstituted CH_2 units and aldehydes (Figure 1c).
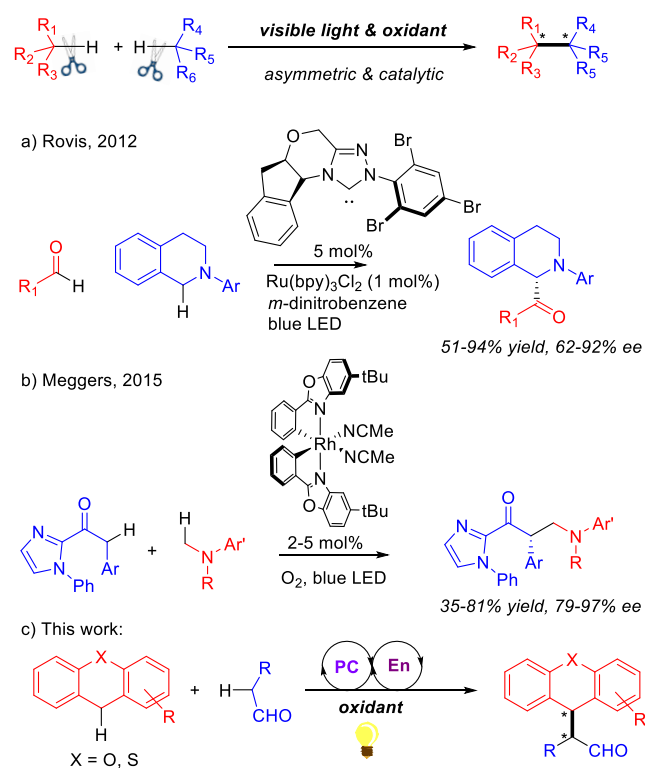

Figure 1. Asymmetric visible-light driven CDC.

We commenced our study by investigating the asymmetric CDC between xanthene **1a** and pentanal **2a** under visible-light photoredox conditions in presence of the Jørgensen's catalyst **cat.1** (Figure 2). The high-throughput experimentation (Figure 2, see SI for more details) allowed us to rapidly screen reaction conditions. We used a 96-well-plate reactor engineered to allow each reaction to be irradiated independently by a single light-emitting diode (LED) to evaluate important reaction parameters.

Screening of solvents (see SI for details) and photocatalysts (Figure 2a) allowed us to identify DCE and Ru(bpy)$_3$Cl$_2$ as an optimal solvent and photocatalyst, correspondingly. We did not observe any reasonable correlation between the reactivity and oxidation/reduction potentials of tested photocatalysts. The Ru(bpy)$_3$ complex seems to have both potentials matching the corresponding electrochemical properties of reagents/intermediates (*vide infra*). Due to a better solubility, Ru(bpy)$_3$(PF$_6$)$_2$ gave slightly better conversion when the reaction was performed on a catalytic scale (0.2 mmol). Screening of different oxidants showed that the presence of a weak C-Br bond is crucial for the reactivity: among different bromoalkanes that were tested BrCCl$_3$ gave the highest conversion to the product. In contrast, other oxidants (O$_2$, CCl$_4$) showed no conversion to the desired product (Figure 2b).
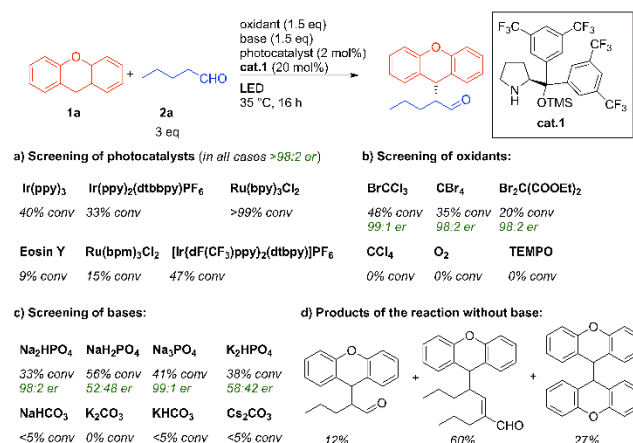

Figure 2. HTE screening of reaction conditions (see details in SI).

Control experiments (Table 1, entries 3-6) showed that light, photocatalyst, base and oxidant are all crucial for achieving an appreciable conversion to the product. Notably, base is required in order to scavenge HBr - a stoichiometric product of the reaction. In support of this hypothesis, in the absence of any base mostly self-condensation products of aldehyde **2a** along with 12% of the desired product were observed in the reaction crude (Figure 2d, see SI for details). Other mild phosphate bases (e.g. NaH$_2$PO$_4$, Na$_2$HPO$_4$) also gave a reasonable conversion, whereas stronger carbonate bases (such as K$_2$CO$_3$, Cs$_2$CO$_3$) were ineffective in the studied reaction (Figure 2c). During the screening of organocatalysts (Table 1, bottom) we found that MacMillan's catalysts **cat.2** and **cat.3** are catalytically active in the studied reaction, however inferior enantioselectivities were observed. Comparison of different prolinol derivatives **cat.4-cat.6** highlights an importance of both TMS protecting group and bis(trifluoromethyl)phenyl substituent for reactivity and enantioselectivity. The loading of **cat.1** can be lowered to 10 mol% without affecting the reaction yield and enantioselectivity (Table 1, entry 2). Finally, when the reaction was performed in the presence of a radical scavenger (Table 1, entry 7), much lower conversion to product was achieved, thus indicating a radical nature of the process (*vide infra*).

The scope of the enantioselective CDC of xanthene with various aldehydes was then extensively investigated under the optimized reaction conditions (Figure 3). Aliphatic aldehydes delivered products in good yields and excellent enantioselectivities (**3a-d**). The more sterically hindered isobutyraldehyde (**2e**) gave product **3e** in 57% yield and 99.5:0.5 er. Thioxanthene (**1b**) was well tolerated in the CDC reaction (**3f**). Substituted phenylpropanals as well as benzyloxy-substituted aldehydes were compatible with the catalytic system (**3g-k**). Surprisingly, product **3k** with a benzyloxy substituent directly attached to the α-carbon of the aldehyde reactant (*i.e.*, to the β-carbon of the enamine intermedi-

ate) was obtained as a racemic mixture.[12] Non-conformationally restricted, electron-rich diarylmethanes (**1l,m**) unfortunately did not give the desired products, probably due to a lower stability of the corresponding radical (*vide infra*).

Table 1. Optimization of reaction conditions and control experiments.

Entry	Variation from standard conditions	Conversion[a], %	Yield[b], %	er[c]
1	-	78	65	97:3
2	10 mol% **cat.1**	76	63	97:3
3	no light	0	n.d.	n.d.
4	no Ru	4	n.d.	97:3
5	no Na$_3$PO$_4$	12	n.d.	97:3
6	no BrCCl3	0	n.d.	n.d.
7	with 1.1 eq. galvynoxyl	26	n.d.	97:3

Reactions performed on 0.2 mmol scale. [a] Conversion was determined by GC analysis. [b] Yield of isolated product. [c] Determined by HPLC analysis using a chiral stationary phase. [d] Results for **cat.2-cat.6** with no variation from standard conditions. n.d.=not determined.
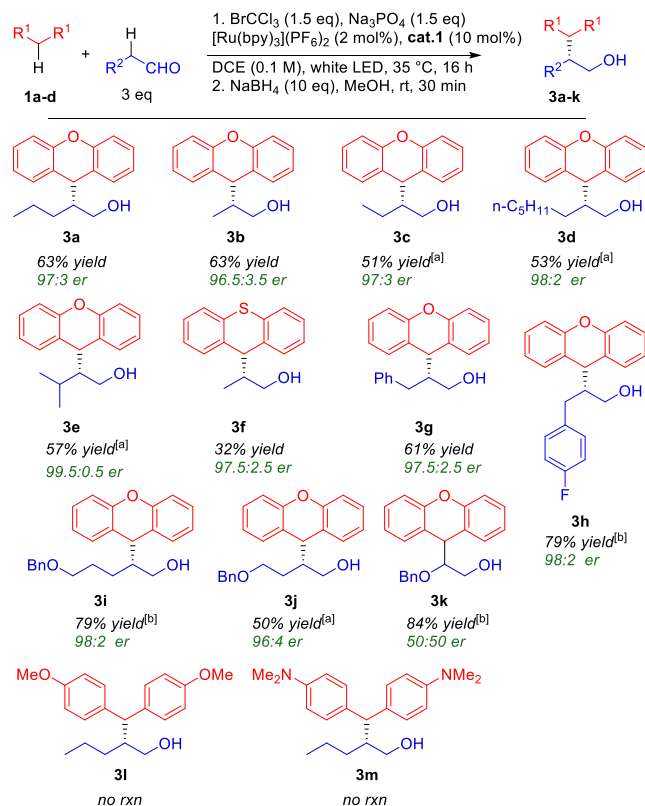

Figure 3. Scope of aldehydes and diarylmethanes in the asymmetric photoredox CDC. Reactions performed on 0.2 mmol scale. [a] With 2 mol% of Ru(bpy)$_3$Cl$_2$. [b] With 20 mol% of **cat.1**.
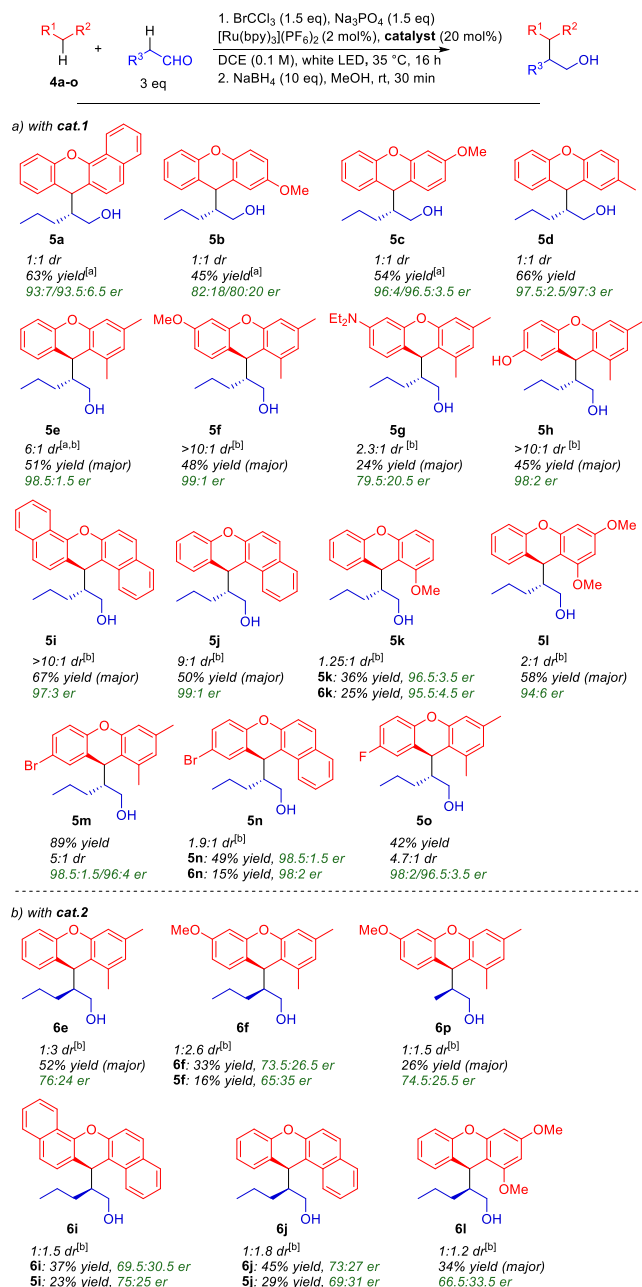
Figure 4. Scope of substituted xanthenes in the asymmetric photoredox CDC. Reactions performed on 0.2 mmol scale. [a] Carried out with 10 mol% **cat.1**. [b] Diastereomeric ratio determined by NMR analysis of the crude reaction mixture, given as **5**/**6** ratio.

Next, different substituted xanthenes were subjected to the photoredox CDC with pentanal (Figure 4a).[13] 2-, 3- and 4-substituted xanthenes delivered the corresponding products in good yields and high enantioselectivities (up to 97.5:2.5 er), but eventually as 1:1 mixtures of diastereomers (**5a-d**). To our delight, the reaction with 1-methyl-substituted xanthenes gave much higher diastereoselectivities (up to 10:1) and in many cases single diastereomers could be easily isolated (**5e-h,m-o**). Products derived from benzo-fused xanthenes (**5i,j,n**) were obtained in good yields and excellent diastereo- and enantioselectivities. On the other side, 1-methoxyxanthenes gave the corresponding products with lower diastereoselectivities (**5k,l**) allowing, however, the isolation of both diastereomers in moderate yields and high enantiomeric

purities. The reaction tolerates different functional groups, such as methoxy, phenolic hydroxyl, diethylamino, bromo, fluoro. This could open up possibilities for the orthogonal functionalization of products by cross-coupling (**5m,n**) or etherification (**5h**).

Interestingly, we found that switching from the Jørgensen's catalyst **cat.1** to MacMillan's catalyst **cat.2** allowed to switch the diastereoselectivity in favor of a different diastereomer, where the configuration of the α-carbon had been inverted (Figure 4b).[14] Several substrate combinations were tested with **cat.2**, affording moderate to good yields of the corresponding products (up to 74% combined yield of diastereomers). Due to the lower diastereoselectivity achieved with this catalyst, the yields of individual diastereomers were relatively moderate. Enantioselectivities with **cat.2** reached the modest level of 76:24 er (for **6e**), and further screening of imidazolinones did not significantly improve this result (*e.g.*, 79:21 er for **6e** with **cat.3**, see SI for more details). In general, in the studied transformation the Jørgensen's catalyst **cat.1** is more selective in terms of enantio- and diastereoselectivity, compared with imidazolinones **cat.2** and **cat.3**. In the case of 1-substituted xanthenes **4e-o** it leads to a stronger catalyst control of diastereoselectivity by **cat.1**, whereas the reaction in presence of **cat.2** is substrate controlled. The absolute configuration of product **5e** was determined by single-crystal X-ray diffraction of its ferrocene derivative.[15] The second diastereomer (**6e**) was crystallized as a racemate, which allowed us to determine its relative configuration (Figure 5).[15]
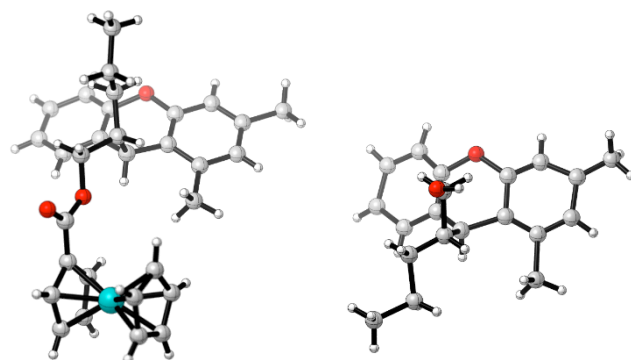

Figure 5. X-ray structure of ferrocene derivative of **5e** (left) and (*rac*)-**6e** (right).

The proposed mechanism for the studied transformation is shown in Figure 6. It consists of two separate catalytic cycles: photoredox and organocatalytic. In the photoredox cycle, bromotrichloromethane ($E_{1/2}$ = -0.18 V vs SCE)[16] is first reduced by the excited state of the Ru(II) complex ($E_{1/2}$ = -0.81 V vs SCE)[17] to the CCl$_3$ radical (oxidative quenching), which then abstracts a hydrogen atom from xanthene **1a** to generate the xanthyl radical **INT1**.[19,20] Suppression of the catalytic reaction in the presence of a radical scavenger (*vide supra*) gave the first evidence for the radical nature of the process. Secondly, an experimentally measured kinetic isotope effect (KIE) of 4.0 indicates that C-H bond cleavage occurs during the rate-limiting step. This was additionally confirmed by DFT study of the reaction mechanism (see SI for more details).[21,22] Calculations show that the hydrogen abstraction step by the CCl$_3$ radical through transition state **TS1** is rate-limiting with an activation barrier $\Delta G^{\ddagger}$ = 8.3 kcal/mol (Figure 6). Moreover, the KIE predicted by computations (4.3) is in a perfect accordance with the experimental value of 4.0.
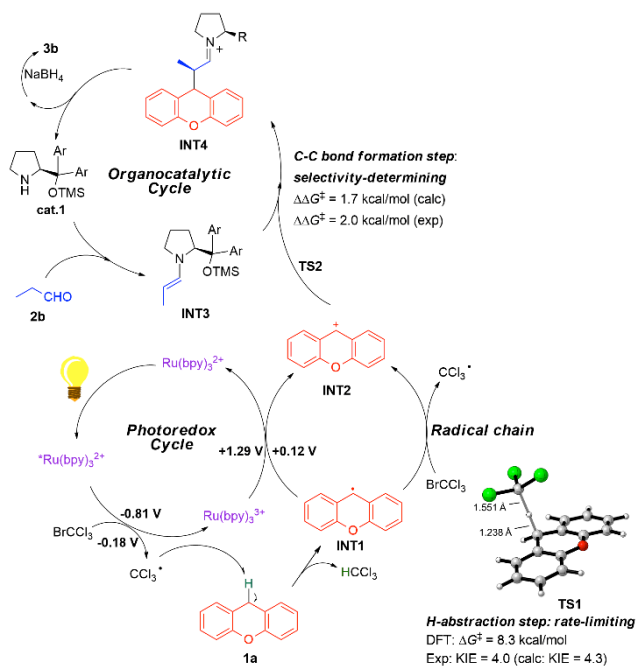
Figure 6. Mechanistic proposal and DFT results. The reduction potentials for BrCCl$_3$,[16] Ru complexes[17] and **INT2**[18] (*vs* SCE) were taken from literature.

Stern-Volmer plot measurements show significant quenching of the excited Ru(bpy)$_3^{2+}$ by BrCCl$_3$ (quenching rate $k_q = 1.5 \times 10^8$ M^{-1} s^{-1}) which is in agreement with the proposed mechanism (Figure 6).[23,24] At this point we cannot exclude a radical chain mechanism where radical **INT1** ($E_{1/2} = 0.12$ V *vs* SCE) would directly reduce BrCCl$_3$ ($E_{1/2} = -0.18$ V *vs* SCE) to a CCl$_3$ radical (Figure 6).[25] In this case photocatalyst is only required in the first cycle to start a chain. The CCl$_3$ radical is then regenerated in a chain propagation step ($\Delta G_{rxn} = +6.9$ kcal/mol).[26]

In the computational study of the C-C bond forming step we considered different possibilities, such as attack of radical **INT1** onto enamine **INT3** (Pathway A in Figure 7, $\Delta G^\ddagger = 20.6$ kcal/mol) or oxidation of enamine **INT3** to the corresponding radical-cation ($E_{1/2} = 0.49$ V *vs* SCE)[27] followed by the attack of **INT1** (Pathway B in Figure 7, $\Delta G^\ddagger = 30.9$ kcal/mol). However, the most energetically favorable pathway was found to be an oxidation of xanthyl radical **INT1** to cation **INT2** ($E_{1/2} = 0.12$ V *vs* SCE)[18] by the Ru(III) complex ($E_{1/2} = 1.29$ V *vs* SCE),[17] followed by the classical attack of so-generated cation on enamine **INT3** *via* transition state **TS2** (Pathway C in Figure 7, $\Delta G^\ddagger = 4.3$ kcal/mol). The latter step is the selectivity-determining, deciding which enantiomer of **INT4** and, correspondingly, of product **3b**, is formed. Computed energy difference between diastereomeric transition states (*R*)-**TS2** and (*S*)-**TS2** ($\Delta\Delta G^\ddagger = 1.7$ kcal/mol) is in a perfect agreement with the experimental data ($\Delta\Delta G^\ddagger = 2.0$ kcal/mol).

We also considered an alternative pathway *via* the reductive quenching of excited Ru(II) species ($E_{1/2} = 0.77$ V *vs* SCE)[17] by enamine **INT3** ($E_{1/2} = 0.49$ V *vs* SCE).[27] This redox step is therefore energetically favorable (see SI for details). The next step, attack of the corresponding radical-cation by radical **INT1**, has however a high activation barrier (Pathway B in Figure 7, $\Delta G^\ddagger = 30.9$ kcal/mol). This pathway is thus less favorable than the oxidative quenching pathway.
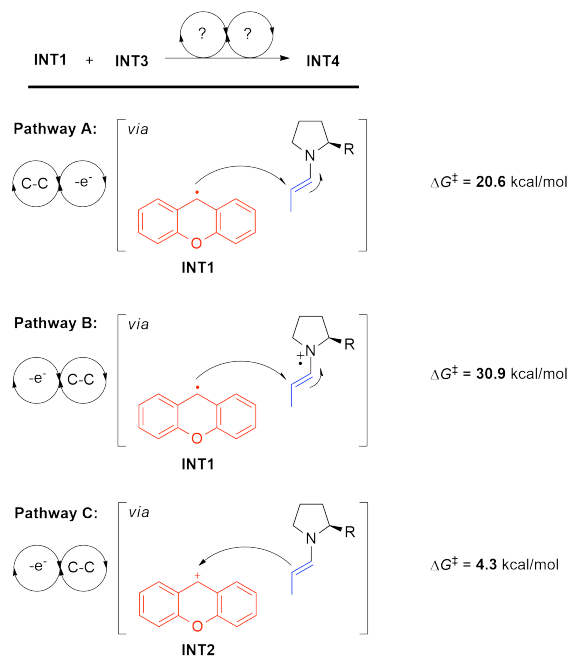

Figure 7. Possible pathways of the C-C bond forming step.

In conclusion, we have developed a unique catalytic asymmetric cross-dehydrogenative coupling of xanthenes and thioxanthenes with aldehydes using visible light as a sustainable source of energy. The reaction features high enantioselectivities, good yields and wide functional group tolerance. The method was extended to the coupling of non-symmetrical xanthenes, which give CDC products with high diastereoselectivities, thus allowing isolation of single diastereomers in good yields and with high enantiomeric purities. Mechanistic studies by experimental and computational methods have shown that the reaction proceeds *via* the rate-limiting hydrogen abstraction followed by single-electron transfer and selectivity-determining attack of cation on enamine. Ongoing studies focus on the further extension of substrate scope in terms of variation of diarylmethane partner and application of this methodology to the synthesis of complex molecules.

AUTHOR INFORMATION

Corresponding Author

*mapericas@iciq.es.

ASSOCIATED CONTENT

Supporting Information

The Supporting Information is available free of charge on the ACS Publications website.

Experimental and computational details (PDF)

ACKNOWLEDGMENT

REFERENCES

[1]   a) Labinger, J. A.; Bercaw, J. E. *Nature* **2002**, 417, 507–514; b) Godula, K.; Sames, D. *Science* **2006**, 312, 67–72; c) Bergman, R. G. *Nature* **2007**, 446, 391–393.

[2]   a) Zhang, S.-Y.; Zhang, F.-M.; Tu, Y.-Q. *Chem. Soc. Rev.* **2011**, 40, 1937–1949: b) Kuhl, N.; Hopkinson, M. N.; Wencel-Delord, J.; Glorius, F. *Angew. Chem.* **2012**, 124, 10382–10401; *Angew. Chem. Int. Ed.* **2012**, *51*, 10236–10254; c) Zheng, C.; You, S.-L. *RSC Adv.* **2014**, 4, 6173–6214.

[3]   For recent reviews on CDC, see: a) Yeung, C. S.; Dong, V. M. *Chem. Rev.* **2011**, 111, 1215–1292; b) Rohlmann, R.; García Mancheño, O. *Synlett* **2013**, 24, 6–10; c) Girard, S. A.; Knauber, T.; Li, C.-J. *Angew. Chem. Int. Ed.* **2014**, 53, 74–100; *Angew. Chem.* **2014**, *126*, 76–103; d) Zhao, Y.-L.; Wang, Y.; Luo, Y.-C.; Fu, X.-Z.; Xu, P.-F. *Tetrahedron Letters* **2015**, 56, 3703–3714.

[4]   a) Murahashi, S.-I.; Zhang, D. *Chem. Soc. Rev.* **2008**, 37, 1490–1501; b) Li, C.-J. *Acc. Chem. Res.* **2009**, 42, 335–344.

[5]   Recent examples of asymmetric CDC: a) Meng, Z.; Sun, S.; Yuan, H.; Lou, H.; Liu, L. *Angew. Chem., Int. Ed.* **2014**, 53, 543–547; b) Perepichka, I.; Kundu, S.; Hearne, Z.; Li, C.-J. *Org. Biomol. Chem.* **2015**, 13, 447–451; c) Xie, Z.; Zan, X.; Sun, S.; Pan, X.; Liu, L. *Org. Lett.* **2016**, 18, 3944–3947; d) Tan, Y.; Yuan, W.; Gong, L.; Meggers, E. *Angew. Chem., Int. Ed.* **2015**, 54, 13045–13048; e) Narute, S.; Pappo, D. *Org. Lett.* **2017**, 19, 2917−2920.

[6]   Recent reviews on photoredox catalysis: a) Narayanam, J. M. R.; Stephenson, C. R. J. *Chem. Soc. Rev.* **2011**, 40, 102–113; b) Prier, C. K.; Rankic, D. A.; MacMillan, D. W. C. *Chem. Rev.* **2013**, 113, 5322–5363; c) Schultz, D. M.; Yoon, T. P. *Science* **2014**, 343, 985; d) Ravelli, D.; Protti, S.; Fagnoni, M. *Chem. Rev.* **2016**, 116, 9850–9913.

[7]   For reviews on C–H bond functionalization reactions by photoredox catalysis, see: a) Shi, L.; Xia, W. *Chem. Soc. Rev.* **2012**, 41, 7687–7697; b) Xie, J.; Jin, H.; Zhu, C. *Tetrahedron Letters* **2014**, 55, 36–48.

[8]   a) Hopkinson, M. N.; Sahoo, B.; Li, J.-L.; Glorius, F. *Chem. Eur. J.* **2014**, 20, 3874–3886; b) Angnes, R. A.; Li, Z.; Correia, C. R. D.; Hammond, G. B. *Org. Biomol. Chem.* **2015**, 13, 9152–9167; c) Skubi, K. L.; Blum, T. R.; Yoon; T. P. *Chem. Rev.* **2016**, 116, 10035–10074.

[9]   a) DiRocco, D. A.; Rovis, T. *J. Am. Chem. Soc.* **2012**, 134, 8094–8097; b) Yang, Q.; Zhang, L.; Ye, C.; Luo, S.; Wu, L.-Z.; Tung, C.-H. *Angew. Chem. Int. Ed.* **2017**, 56, 3694–3698; c) Kumar, G.; Verma, S.; Ansari, A.; Khan, N. H.; Kureshy, R. I. *Catal. Commun.* **2017**, 99, 94–99.

[10]   a) Nagib, D. A.; Scott, M. E.; MacMillan, D. W. C. *J. Am. Chem. Soc.* **2009**, 131, 10875–10877; b) for a recent review on asymmetric catalysis by visible-light activation, see: Meggers, E. *Chem. Commun.* **2015**, 51, 3290–3301.

[11]   a) Benfatti, F.; Capdevila, M. G.; Zoli, L.; Benedetto, E.; Cozzi, P. G. *Chem. Commun.* **2009**, 5919–5921; b) Ho, X. H.; Mho, S. I.; Kang, H.; Jang, H. Y. *Eur. J. Org. Chem.* **2010**, 4436–4441; c) Zhang, B.; Xiang, S.-K.; Zhang, L. H.; Cui, Y.; Jiao, N. *Org. Lett.* **2011**, 13, 5212–5215; d) Huang, F.; Xu, L.; Xiao, J. *Chin. J. Chem.* **2012**, 30, 2721–2725.

[12]   We think the highly electron-rich nature of the enamine intermediate could be responsible for this behavior by triggering a non-enantioselective pathway with participation of the derived radical-cation.

[13]   Substituted xanthenes were prepared according to: Böb, E.; Hillringhaus, T.; Nitsch, J.; Klussmann, M. *Org. Biomol. Chem.* **2011**, 9, 1744 – 1748.

[14]   Although catalysts **cat.1**, **cat.2** and **cat.3** gave the same configuration of the α-carbon atom in the product **3a** (Table 1), an opposite configuration of the α-carbon atom in products **5** and **6** was observed when catalyst **cat.2** was employed (Figure 4). This side-differentiation change could be caused by the increased size of the substituents at the xanthene partner.

[15]   CCDC 1511524 and 1511523 for ferrocene derivative of **5e** and (*rac*)-**6e**, respectively, contain the supplementary crystallographic data for this article. These data can be obtained free of charge from The Cambridge Crystallographic Data Centre (CCDC) at www.ccdc.cam.ac.uk/data_request/cif.

[16]   Murayama, E.; Kohda, A.; Sato, T. *J. Chem. Soc., Perkin Trans.* **1980**, 1, 947–949.

[17]   Kalyanasundaram, K. *Coord. Chem. Rev.* **1982**, 46, 159–244.

[18]   Zhu, X.-Q.; Dai, Z.; Yu, A.; Wu, S.; Cheng, J.-P. *J. Phys. Chem. B* **2008,** 112*,* 11694–11707.

[19]   The second product of this step, $CHCl_3$ was detected in the crude reaction mixture (see SI for more details).

[20]   Radical **INT1** is additionally stabilized by the conjugation with the adjacent aromatic rings. This could explain the non-reactivity of the non-cyclic substrates (**1l,m**) (see Figure 3) where the corresponding **INT1** would lack such a stabilization.

[21]   DFT method: PCM_{DCE}-B2PLYP-D3/6-311+G(d,p)//B3LYP/6-31G(d).

[22]   Frisch, M. J.; Trucks, G. W.; Schlegel, H. B.; Scuseria, G. E.; Robb, M. A.; Cheeseman, J. R.; Scalmani, G.; Barone, V.; Mennucci, B.; Petersson, G. A.; Nakatsuji, H.; Caricato, M.; Li, X.; Hratchian, H. P.; Izmaylov, A. F.; Bloino, J.; Zheng, G.; Sonnenberg, J. L.; Hada, M.; Ehara, M.; Toyota, K.; Fukuda, R.; Hasegawa, J.; Ishida, M.; Nakajima, T.; Honda, Y.; Kitao, O.; Nakai, H.; Vreven, T.; Montgomery, J. A., Jr.; Peralta, J. E.; Ogliaro, F.; Bearpark, M.; Heyd, J. J.; Brothers, E.; Kudin, K. N.; Staroverov, V. N.; Kobayashi, R.; Normand, J.; Raghavachari, K.; Rendell, A.; Burant, J. C.; Iyengar, S. S.; Tomasi, J.; Cossi, M.; Rega, N.; Millam, J. M.; Klene, M.; Knox, J. E.; Cross, J. B.; Bakken, V.; Adamo, C.; Jaramillo, J.; Gomperts, R.; Stratmann, R. E.; Yazyev, O.; Austin, A. J.; Cammi, R.; Pomelli, C.; Ochterski, J. W.; Martin, R. L.; Morokuma, K.; Zakrzewski, V. G.; Voth, G. A.; Salvador, P.; Dannenberg, J. J.; Dapprich, S.; Daniels, A. D.; Farkas, Ö.; Foresman, J. B.; Ortiz, J. V.; Cioslowski, J.; Fox, D. J. Gaussian 09, Revision D.01; Gaussian, Inc., Wallingford, CT, 2009.

[23]   Cismesia, M. A.; Yoon, T. P. *Chem. Sci.* **2015**, 6, 5426–5434.

[24]   From the other side, a significant quenching rate k_q by xanthene **1a** (2.3×10^8 M^{-1} s^{-1}) was observed. It is unlikely to be caused by direct oxidation of **1a** to the corresponding radical cation due to the high value of the corresponding potential: $E_{1/2}$ = 1.55 V *vs* SCE (see ref 25).

[25]   The quantum yield measurements would be helpful to clarify this scenario, but they were not possible due to the heterogeneity of the reaction mixture.

[26]   Alternative radical chain pathway *via* the addition of radical **INT1** onto enamine **INT3**, followed by the reduction of $BrCCl_3$ by the formed intermediate, is also feasible. However, according to further discussion this pathway would have a higher activation barrier (20.6 kcal/mol, Pathway A on Figure 7).

[27]   Reduction potential from DFT calculations, see SI for details.

TOC graphics:
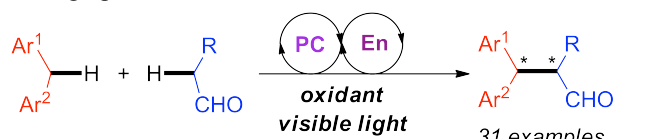
- *Enantio- and diastereoselective*
- *Mild conditions*
- *Broad substrate scope*
- *Mechanistic study (expt + DFT)*

31 examples
up to 89% yield
up to 99.5:0.5 er